

LEVEL-SET FORMULATION BASED ON OTSU METHOD WITH MORPHOLOGICAL REGULARIZATION

Jeová F. S. R. Neto, Alan M. Braga, Fátima N. S. de Medeiros

Regis C. P. Marques

Vision, Image and Systems Laboratory
Federal University of Ceará
Fortaleza, Brazil

Telematics Department
Federal Institute of Technology of Ceará
Fortaleza, Brazil

ABSTRACT

Noisy image segmentation is one of the most important and challenging problem in computer vision. In this paper, we propose a level set segmentation technique inspired by the classic Otsu thresholding method. The front propagation of the proposed level set based method embeds a cost function that takes into account first-order statistical moments. In order to deal with highly noisy images, we also added a morphological step to our algorithm which led the final segmentation more robust and efficient. Tests were carried out on images artificially contaminated with Gaussian and Salt & Pepper noise patterns. The results showed that our methodology outperformed the classic Otsu thresholding algorithm and an active contour based technique in terms of the Error of Segmentation (EoS), Rate of False Positive (RFP), Rate of False Negative (RFN) and Dice evaluation measures. In addition, the designed algorithm attained a lower average computational time when compared to the active contour related method.

Index Terms— Image segmentation, Level set methods, Otsu thresholding

1. INTRODUCTION

Region-based segmentation methods divide an image into multiple parts according to its semantic or visual characteristics. This task finds applications in biomedical areas [1, 2], synthetic aperture radar (SAR) imagery [3, 4], object recognition [5] and video processing [6], to name a few. In order to accomplish an efficient and reliable automatic region separation, several methodologies have been developed along the past decades. Strategies using histogram-based algorithms [7], graph cuts [8] and variational methods [9, 10] are able to provide good solutions for different segmentation schemes.

However, the main problem involving image partitioning into regions is the presence of noise whose origin may vary from the image formation and transmission phenomena to compression aspects. The primary approach to tackle this problem relies on noise filtering which adds extra computational effort to the overall algorithm and it also leads to information loss. On the other hand, several statistical models

have been also used in segmentation algorithms in order to statistically deal with noisy image [3, 11]. Nevertheless, they were only successfully applied to specific types of images and noise patterns. This is the main reason why it is difficult to develop a general segmentation methodology to deal with any type of noise. In fact, the design of such methodology is therefore highly desired.

The well-known Otsu thresholding algorithm [7] embodies image statistics extracted from its histogram to attain a general statistical-based methodology. Although it is not robust to any kind of noise, the Otsu algorithm is useful to develop and support other segmentation methods [11]. Level Set based methods [12, 13] brought up satisfactory results on the segmentation of very noisy images [14]. In addition, these methods can be adapted to embody different functionals and cost functions.

This paper introduces a level set based scheme that encompasses the Otsu cost function to drive the front propagation. Differently from other approaches that use the Otsu algorithm as a part of the level set formulation [15], we designed a cost function based on its criterion for image partitioning to guide the curve evolution. Within such approach, our level set segmentation algorithm incorporates image statistics independent of the mathematical noise modeling to attain satisfactory results with noisy images. We added a morphological step to the algorithm with the aim of regularizing the front temporal development. Furthermore, it achieves a fast curve evolution, particularly when compared with the active contour based method.

The remainder of the this paper is organized as follows. Section 2 reviews the Otsu thresholding algorithm and the corresponding cost function while Section 3 presents the level set approach. Section 4 introduces the proposed level set model. Then, Section 5 presents the assessment methodology and some qualitative and quantitative experimental segmentation results on noisy images. Finally, Section 6 concludes the paper and presents further work.

2. OTSU THRESHOLDING AND ITS COST FUNCTION

A thresholding-based algorithm searches for the best threshold to partition a gray-level image histogram and hence it generates a binary image. It is defined as

$$I_s(x, y) = \begin{cases} 1 & \text{if } I(x, y) > T \\ 0 & \text{if } I(x, y) \leq T \end{cases}, \quad (1)$$

where the threshold T separates the image gray levels into two regions and the segmentation result or binarization is $I_s(x, y)$.

A well-known thresholding algorithm was introduced by Otsu [7] to search for the best threshold value and it is based on the following measure:

$$\sigma_{\text{inner}}^2(T) = w_0(T)\sigma_0^2(T) + w_1(T)\sigma_1^2(T), \quad (2)$$

where $w_0(T)$ and $w_1(T)$ stand for the probabilities of a pixel to belong to the region 0 or 1, respectively, when applying the threshold T to an image histogram. $\sigma_0^2(T)$ and $\sigma_1^2(T)$ are the variances of each segmented region. Thus, the algorithm achieves the segmentation result when it minimizes the value of the inner variance ($\sigma_{\text{inner}}^2(T)$). According to this approach, an optimal segmentation threshold for a grayscale image is given by

$$T_{\text{optimal}} = \arg \min_{0 < T < 255} \sigma_{\text{inner}}^2(T). \quad (3)$$

3. LEVEL SETS

The level set approach [12] is an efficient tool for numerical computation of moving interfaces. Within this approach, a front $\vec{\phi} : \mathbb{R}^2 \times \mathbb{R}^+ \rightarrow \mathbb{R}$ changes and adapts its morphology to attain a desired minimal energy state. This front is defined as the level-set zero of a surface $\psi(\mathbf{x}, t)$ embedded on a higher dimensional space. It is given by,

$$\vec{\phi}(s, t) = \{\mathbf{x} | \psi(\mathbf{x}, t) = 0\}, \quad \mathbf{x} \in \mathbb{R}^n, \quad (4)$$

where $s \in \mathbb{R}^2$ corresponds to the coordinates of the parametrized curve and $t \in \mathbb{R}^t$ represents the evolution time.

The front evolves in accordance with a given cost function \mathcal{C} which governs the surface $\psi(\mathbf{x}, t)$ motion. Such process is evaluated using the Euler-Lagrange descent equation [12] with respect to \mathcal{C} . Therefore, the front propagation is obtained by [12]:

$$\frac{d\vec{\phi}}{dt} = -\frac{\partial \mathcal{C}}{\partial \vec{\phi}}, \quad (5)$$

where $\frac{\partial \mathcal{C}}{\partial \vec{\phi}}$ is the functional derivative of the cost function \mathcal{C} with respect to the curve $\vec{\phi}$.

From Eq. 5, a level set model with a front velocity function F may be derived using \mathcal{C} . Thus, the temporal evolution of the front can be rewritten as [16]:

$$\frac{d\vec{\phi}}{dt} = F|\nabla \psi(\mathbf{x}, t)|, \quad (6)$$

where $|\nabla(\cdot)|$ denotes the gradient norm of a vector-valued function. In fact, the front propagation model and the velocity function are closely related to the cost function definition. From Eq. 6, the surface evolution equation is defined as:

$$\psi_{n+1} = \psi_n + F|\nabla \psi_n|\Delta t, \quad (7)$$

where Δt is the time step and ψ_n is the level set function in the n -th step.

4. PROPOSED FRONT PROPAGATION MODEL

4.1. Initial Level Set

Inspired by [7], our method encompasses a cost function (Eq. 2) to drive the front evolution. Considering that a level set front spatially divides a given image into two regions, i.e. inside the front (where $\psi(\mathbf{x}, t) > 0$) and outside it (where $\psi(\mathbf{x}, t) < 0$). Thus, we propose the following cost function to drive the front evolution:

$$\mathcal{C}(\vec{\phi}) = w_{R_i}(\vec{\phi})\sigma_{R_i}^2(\vec{\phi}) + w_{R_o}(\vec{\phi})\sigma_{R_o}^2(\vec{\phi}), \quad (8)$$

where R_i and R_o represent the regions inside and outside the front, respectively, and $\vec{\phi}$ refers to the region boundaries. $\sigma_{R_i}^2(\vec{\phi})$ and $\sigma_{R_o}^2(\vec{\phi})$ provide the grayscale intensity variances for each image region and w_{R_i} and w_{R_o} correspond to the respective areas of both regions. Note that our proposed cost criterion deals with the weighted inner variance to discriminate the regions present in the image.

The sample variance is given by:

$$\sigma_R^2(\vec{\phi}) = \frac{\int_R (I(\mathbf{x}) - \mu_R)^2 d\mathbf{x}}{\int_R d\mathbf{x}}, \quad (9)$$

where μ_R is the mean grayscale intensity of the region R . Since the denominator in Eq. 9 is the area of R , Eq. 8 can be rewritten as:

$$\mathcal{C}(\vec{\phi}) = \int_{R_i} (I(\mathbf{x}) - \mu_{R_i})^2 d\mathbf{x} + \int_{R_o} (I(\mathbf{x}) - \mu_{R_o})^2 d\mathbf{x}. \quad (10)$$

According to Eq. 3, the optimal boundary, i. e., the final segmentation is given by:

$$\vec{\phi}_{\text{optimal}} = \arg \min \mathcal{C}(\vec{\phi}). \quad (11)$$

Thus, we derived a new front propagation from Eq. 5:

$$\begin{aligned} \frac{d\vec{\phi}}{dt} &= -\frac{\partial \mathcal{C}(\vec{\phi})}{\partial \vec{\phi}} = -\left[\sum_{n=i,o} \frac{\partial}{\partial \vec{\phi}} \int_{R_n} (I(\mathbf{x}) - \mu_{R_n})^2 d\mathbf{x} \right] \\ &= [(I(\mathbf{x}) - \mu_{R_i})^2 - (I(\mathbf{x}) - \mu_{R_o})^2] \vec{n}, \end{aligned} \quad (12)$$

where \vec{n} is the unit vector that arises normally to the level set front [17]. The minus signal is due to the normal vectors of both regions which present opposite directions. From Eq. 6 and Eq. 12, we derive Eq. 13 which is the proposed level set temporal equation.

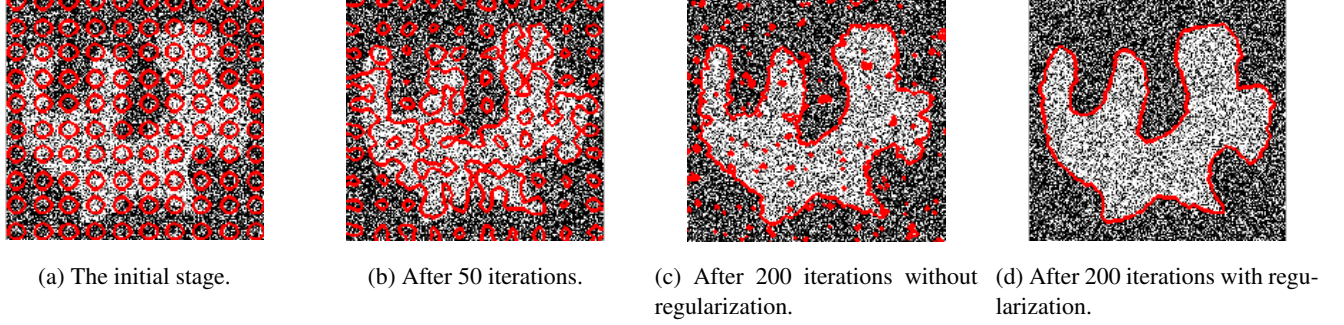


Fig. 1: Segmentation results of our method applied to an image contaminated with the Gaussian noise ($\mu_g = 0$, $\sigma_g^2 = 1$).

4.2. Morphological Regularization

In order to tackle with very high noisy images, the proposed approach also embodies morphological operators and applies them, at each evolution step, to the $\psi(\mathbf{x}, t)$ surface for image enhancement. Thus, the proposed surface evolves as:

$$\psi_{n+1} = [(\psi_n + F|\nabla\psi_n|\Delta t) \circ S] \bullet S, \quad (13)$$

where \circ and \bullet represent the opening and closing morphological operations, respectively, and S is the structural element. Thus, our algorithm efficiently deals with very noisy regions on the image which can be incorrectly interpreted as new regions to segment, since the cost function (Eq. 8) evokes the inner variance as the main criterion to differentiate segmented regions. With these morphological operations, small regions are not considered in the segmentation process and therefore the final algorithm becomes more robust to noisy data.

5. RESULTS AND DISCUSSIONS

5.1. Assessment Methodology

For performance evaluation of the segmentation techniques, we applied the Error of Segmentation (EoS) which is defined as [11]:

$$\text{EoS} = \frac{\#(A)}{\#(Image)}, \quad (14)$$

where $\#(A)$ and $\#(Image)$ are the number of misclassified pixels and the number of pixels of the image, respectively. We also assessed the results with the Rate of False Positive (RFP), Rate of False Negative (RFN) and Dice [19, 20] measures given by:

$$\text{RFP} = \frac{|S - (R \cap S)|}{|R|}, \quad (15)$$

$$\text{RFN} = \frac{|R - (R \cap S)|}{|R|}, \quad (16)$$

$$\text{Dice} = \frac{2|R \cap S|}{|R| + |S|}, \quad (17)$$

where R and S are the ground truth and the segmented images, respectively.

The proposed algorithm was compared with the Otsu thresholding technique [7] and an active contour based method (AC) [18]. We have chosen these methods for comparison assessment because the former inspired us to design the proposed cost function to drive the front evolution and the latter is a related variational segmentation method.

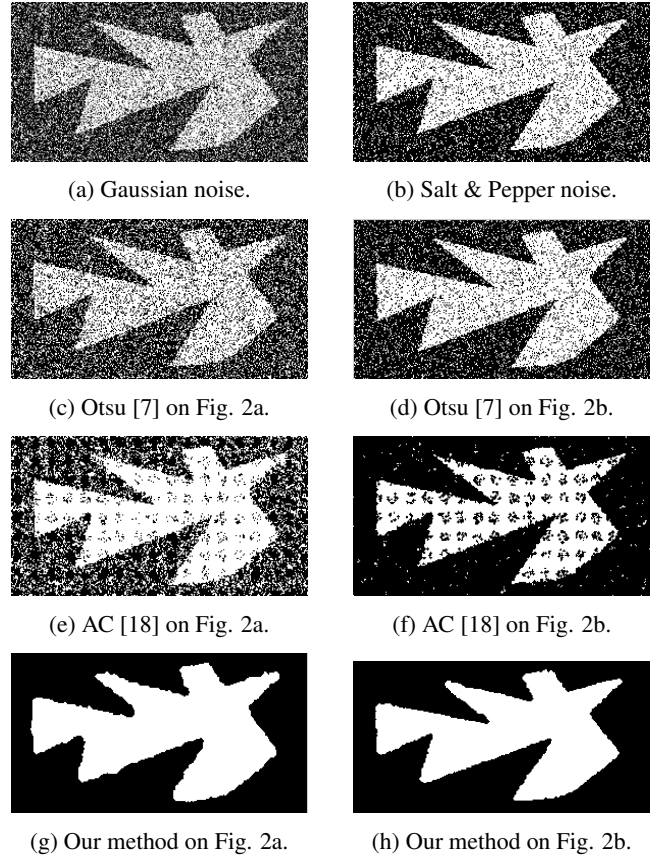





Fig. 2: Contaminated images and the corresponding segmentation results. Salt & Pepper noise ($d = 0.3$) and Gaussian noise ($\mu_g = 0$, $\sigma_g = 0.5$).

Table 1: Average metrics^a over 100 segmentation runs on synthetically contaminated images following the three shape patterns.

											
Noise Type	Noise Parameters		Proposed	Otsu [7]	AC [19]	Proposed	Otsu [7]	AC [19]	Proposed	Otsu [7]	AC [19]
EoS ↓	Gaussian	$\mu_g = 0, \sigma_g^2 = 0.5$	0.0054	0.2464	0.1938	0.0102	0.2513	0.2622	0.0246	0.2504	0.1175
		$\mu_g = 0, \sigma_g^2 = 1$	0.0110	0.3118	0.2649	0.0204	0.3133	0.3436	0.0426	0.3133	0.1637
	Salt & Pepper	$d = 0.3$	0.0025	0.1502	0.0737	0.0043	0.1500	0.1265	0.0079	0.1502	0.0915
		$d = 0.7$	0.0110	0.3501	0.3134	0.0201	0.3502	0.3687	0.0426	0.3501	0.2278
Dice ↑	Gaussian	$\mu_g = 0, \sigma_g^2 = 0.5$	0.9891	0.6136	0.7053	0.9724	0.5379	0.5760	0.9371	0.5549	0.7319
		$\mu_g = 0, \sigma_g^2 = 1$	0.9778	0.5312	0.6205	0.9433	0.4563	0.5003	0.8856	0.4730	0.6259
	Salt & Pepper	$d = 0.3$	0.9950	0.7412	0.8575	0.9887	0.6805	0.7466	0.9805	0.6944	0.7710
		$d = 0.7$	0.9783	0.4843	0.5601	0.9568	0.4110	0.4626	0.8961	0.4273	0.5246
RFN ↓	Gaussian	$\mu_g = 0, \sigma_g^2 = 0.5$	0.0193	0.2266	0.1123	0.0450	0.2222	0.0530	0.0985	0.2232	0.2018
		$\mu_g = 0, \sigma_g^2 = 1$	0.0407	0.3019	0.1654	0.0969	0.3010	0.0878	0.1779	0.3004	0.3184
	Salt & Pepper	$d = 0.3$	0.0025	0.1502	0.1517	0.0050	0.1502	0.0669	0.0096	0.1506	0.2283
		$d = 0.7$	0.0184	0.3503	0.2185	0.0500	0.3501	0.1588	0.0865	0.3501	0.3717
RFP ↓	Gaussian	$\mu_g = 0, \sigma_g^2 = 0.5$	0.0022	0.7474	0.6537	0.0091	1.1140	1.3413	0.0226	1.0228	0.3827
		$\mu_g = 0, \sigma_g^2 = 1$	0.0029	0.9304	0.8815	0.0116	1.3651	1.7344	0.0342	1.2587	0.4951
	Salt & Pepper	$d = 0.3$	0.0075	0.4434	0.1396	0.0177	0.6476	0.6055	0.0298	0.5969	0.2268
		$d = 0.7$	0.0253	1.0337	1.0203	0.0567	1.5122	1.8015	0.1254	1.3921	0.7617
Average computational time (s)			3.1668	0.0094	7.9791	3.1342	0.0093	8.3795	3.1066	0.0093	4.9421

^aThe symbol ↑ stands for "the greater the measure, the better the result". Similarly, the symbol ↓ represents the opposite.

5.2. Results and Discussion

The experiments were carried out on images synthetically contaminated with additive Gaussian (mean μ_g and variance σ_g^2) and Salt & Pepper (noise density d) noises. Fig. 1 shows some steps of our level set based technique performing on a contaminated image with the Gaussian noise. It also illustrates how the algorithm performs and evolves towards the shape boundary after 200 iterations with and without the morphological regularization. Fig. 2 illustrates the qualitative evaluation of the proposed method, the Otsu thresholding [7] and the active contour (AC) based method [18]. Our method removed remaining artifacts during the level set evolution and therefore attained promising results.

Table 1 presents the quantitative evaluation of the segmentation methods using the measures presented in Section 5.1. The experiments were carried out on tree different shapes with 256×256 pixels and contaminated according to the noisy patterns described in Table 1. The proposed level set and the active contour based algorithms were set with $\Delta t = 0.1$ and the initial front following the pattern exhibited in Fig. 1a. Moreover, we have applied a disk-shaped structuring element (radius equal to 1 pixel) for morphological image enhancement. We followed the level set implementation in [21] and the source code can be accessed in github.com/jeovafarias/LevelSetOtsu. Furthermore, the algorithms were implemented in MATLAB® and executed in a

Intel® Core™ I7-4500u processor with 8 Gb RAM.

These results demonstrated that the proposed methodology achieved good results when compared to the other methods. The level set method iteratively adjusted the cost function to guide the front evolution and deal with different noise patterns, successfully. Regarding the average computational time, the proposed method was faster than AC, although it embodied morphological operations. Finally, these operations added an extra computational effort to the proposed algorithm, but they improved quantitatively and qualitatively the segmentation process at each iteration.

6. CONCLUSION

In this paper, we presented a novel level set technique for image segmentation inspired by the Otsu thresholding algorithm. We designed a technique that successfully adapts a cost function to a moving surface in order to generate a fast and efficient level set propagation front. Our approach achieved good results in the presence of noise. Furthermore, it outperformed the Otsu thresholding algorithm and an active contour based segmentation method.

Further work will mainly extend our technique by considering higher statistical moments and applying it to real and speckled images.

7. REFERENCES

- [1] Dzung L. Pham, Chenyang Xu, and Jerry L. Prince, "Current methods in medical image segmentation 1," *Annual Review of Biomedical Engineering*, vol. 2, no. 1, pp. 315–337, 2000.
- [2] Jinming Duan, Christopher Tench, Irene Gottlob, Frank Proudlock, and Li Bai, "Optical coherence tomography image segmentation," in *IEEE International Conference on Image Processing (ICIP)*. IEEE, 2015, pp. 4278–4282.
- [3] Margarida Silveira and Sandra Heleno, "Water/land segmentation in *sar* images using level sets," in *IEEE International Conference on Image Processing (ICIP)*. IEEE, 2008, pp. 1896–1899.
- [4] Jilan Feng, Zongjie Cao, and Yiming Pi, "Multiphase SAR image segmentation with-statistical-model-based active contours," *IEEE Transactions on Geoscience and Remote Sensing*, vol. 51, no. 7, pp. 4190–4199, 2013.
- [5] Koen E. A. Van de Sande, Jasper R. R. Uijlings, Theo Gevers, and Arnold WM Smeulders, "Segmentation as selective search for object recognition," in *IEEE International Conference on Computer Vision (ICCV)*. IEEE, 2011, pp. 1879–1886.
- [6] Haoqian Wang, Bowen Deng, Kai Li, Yongbing Zhang, and Lei Zhang, "Automatic foreground extraction in video," in *IEEE International Conference on Acoustics, Speech and Signal Processing (ICASSP)*. IEEE, 2014, pp. 6553–6557.
- [7] Nobuyuki Otsu, "A threshold selection method from gray-level histograms," *Automatica*, vol. 11, no. 285–296, pp. 23–27, 1975.
- [8] Wenbing Tao, Hai Jin, and Liman Liu, "A new image thresholding method based on graph cuts," in *2007 IEEE International Conference on Acoustics, Speech and Signal Processing-ICASSP'07*. IEEE, 2007, vol. 1, pp. I–605.
- [9] Chunming Li, Chenyang Xu, Changfeng Gui, and Martin D. Fox, "Distance regularized level set evolution and its application to image segmentation," *IEEE Transactions on Image Processing*, vol. 19, no. 12, pp. 3243–3254, 2010.
- [10] Ying Gu, Wei Xiong, Li-Lian Wang, Jierong Cheng, Weimin Huang, and Jiayin Zhou, "A new approach for multiphase piecewise smooth image segmentation," in *IEEE International Conference on Image Processing (ICIP)*. IEEE, 2014, pp. 4417–4421.
- [11] Francisco. A. A. Rodrigues, Jeová F. S. Rocha Neto, Regis C. P. Marques, Fátima. N. Sombra de Medeiros, and Juvencio S. Nobre, "SAR image segmentation using the roughness information," *IEEE Geoscience and Remote Sensing Letters*, vol. 13, no. 2, pp. 132–136, 2016.
- [12] James A. Sethian, *Level set methods and fast marching methods: evolving interfaces in computational geometry, fluid mechanics, computer vision, and materials science*, vol. 3, Cambridge university press, 1999.
- [13] Lingfeng Wang and Chunhong Pan, "Explicit order model for region-based level set segmentation," in *IEEE International Conference on Acoustics, Speech and Signal Processing (ICASSP)*. IEEE, 2015, pp. 927–931.
- [14] Pascal Martin, Philippe R. Gier, François Goudail, and Frédéric Guérault, "Influence of the noise model on level set active contour segmentation," *IEEE Transactions on Pattern Analysis and Machine Intelligence*, vol. 26, no. 6, pp. 799–803, 2004.
- [15] Juying Huang, Fengzeng Jian, Hao Wu, and Haiyun Li, "An improved level set method for vertebra CT image segmentation," *Biomedical Engineering Online*, vol. 12, no. 1, pp. 48, 2013.
- [16] B. Huang, H. Li, and X Huang, "A level set method for oil slick segmentation in SAR images," *International Journal of Remote Sensing*, vol. 26, no. 6, pp. 1145–1156, 2005.
- [17] Amar Mitiche and Ismail B. Ayed, *Variational and level set methods in image segmentation*, vol. 5, Springer Science & Business Media, 2010.
- [18] Tony F. Chan and Luminita A. Vese, "Active contours without edges," *IEEE Transactions on image processing*, vol. 10, no. 2, pp. 266–277, 2001.
- [19] Lee R. Dice, "Measures of the amount of ecologic association between species," *Ecology*, vol. 26, no. 3, pp. 297–302, 1945.
- [20] Mohammadreza Yadollahi, Aleš Procházka, Magdaléna Kašparová, Oldřich Vyšata, and Vladimír Mařík, "Separation of overlapping dental arch objects using digital records of illuminated plaster casts," *BioMedical Engineering OnLine*, vol. 14, no. 1, pp. 1–15, Jul. 2015.
- [21] Alan. M. Braga, Regis. C. P. Marques, Francisco. A. A. Rodrigues, and Fátima. N. S. Medeiros, "A median regularized level set for hierarchical segmentation of sar images," *IEEE Geoscience and Remote Sensing Letters*, vol. PP, no. 99, pp. 1–5, 2017.